Single and multiband THz metamaterial polarisers

BAGVANTH REDDY SANGALA[1,2,*], ARVIND NAGARAJAN[1], PRATHMESH DESHMUKH[1],
HARSHAD SURDI[1], GOUTAM RANA[3], VENU GOPAL ACHANTA[1] and S S PRABHU[1]

[1]Department of Condensed Matter Physics, Tata Institute of Fundamental Research, Mumbai 400 005, India
[2]Department of Physics, P.G. Centre at Wanaparthy, Palamuru University, Mahbubnagar 509 001, India
[3]Department of Electrical Engineering, Indian Institute of Technology Bombay, Powai, Mumbai 400 076, India
*Corresponding author. E-mail: bagvanthreddy.physicist@gmail.com

Abstract. We report single and multiband linear polarisers for terahertz (THz) frequencies using cut-wire metamaterials (MM). The MMs were designed by finite-element method (FEM), fabricated by electron beam lithography, and characterised by THz time-domain spectroscopy. The MM unit cells consist of single or multiple length cut-wire pads of gold on semi-insulating gallium arsenide (GaAs) for single or multiple band polarisers. For example, a MM with a square unit cell of 50 μm size on 1 mm GaAs substrate with a gold cut wire of 65 μm length, 2 μm width, and 150 nm height gives a resonance around 1.05 THz. The dependence of the resonance frequency of the single-band polariser on the length of the cut-wires was explained based on transmission line model.

1. Introduction

Linear polarisers are used to select light with electric field oscillations confined to a single plane. A combination of two polarisers can attenuate the light intensity in controlled fashion. In the terahertz (THz) part of the electromagnetic spectrum, the commercially available devices for this purpose are wire grid polarisers (WGP) [1]. The WGPs can be free-standing or grown on a substrate [2]. Linear polarisers were also reported using liquid crystals [3], aligned single wall carbon nanotubes [4], Brewster angle silicon wafers [5], aligned nickel nanoparticles [6], etc. With the motivation of making the WGPs robust and inexpensive, some ideas are reported recently [7–9] and even more inexpensive options using gold colour lines printed on a paper [10], silver nanoparticle ink printer on a paper [11], graphite–lead grids on a sheet of paper [12], etc. were reported. All of these devices work for broad spectrum in THz. For a narrow pass-band polariser with better extinction coefficient, antireflection coating on the WGPs seems to be the option [2]. Other than this, there is no direct device that can work as narrow single-band or multiband linear polariser in the entire electromagnetic spectrum.

A cut-wire metamaterial (MM) is a modification of the line grid polariser with an electrical dipole resonance when the incident THz radiation has polarisation along the wires and flat spectral response for orthogonal polarisation and it can work as a narrow-band polariser [13]. A similar type of MM was shown to convert a broadband linear polarised THz radiation into the orthogonal polarisation state [14]. Single-layer cut-wire MMs [15] or pair of cut-wires [16,17] or pair of cut-wire crosses [18] were proposed to realise negative refraction of radiation. A pair of cut-wire crosses was proposed to realise birefringent MMs [19], and high refractive index MM [20]. Tunability of THz transmission using cut-wire or cut-wire-like MMs was reported using temperature-tunable substrates [21] or mechanical-tunable substrates [22]. Metallic cut-wires were also used in realising the perfect absorption [23,24]. Recently, a graphene cut-wire MM was also proposed for narrow-band THz absorption [25], extreme sensitive polariser based on cut-through MM [26], flexible [27] and robust [28] WGP were reported but they are for broad-band frequencies. Three-dimensional MM [29] based and wire grid [30] polarisers were also reported. Short laser pulses are used to generate broad-band THz using photoconductive antennae, optical rectification or intense laser interaction

with matter [31]. While for short pulse studies involving carrier dynamics, one would need broad-band components, for spectroscopic studies, it is essential to have narrow-band filters, polarisers, and other THz components to spectrally resolve resonances. In this work, we explore the narrow-band polarisation property of the cut-wires through finite-element method (FEM) simulations and apply a transmission line model to explain the dependence of resonance frequency on the length of the cut-wires. We demonstrate narrow single-band and multiband polarisers based on THz MMs with the unit cell consisting of a single cut-wise or multiple cut-wires.

2. Design and theoretical consideration

The unit cell of a narrow-band THz polariser is shown in figure 1a. It has gold cut-wires on semi-insulating gallium arsenide (SI-GaAs). Here, the length (L), width (W), and height (h) of the gold cut-wire pad are optimised to 65 μm, 2 μm, and 150 nm, respectively and the period $P = 50$ μm. We designed it using the radio frequency module of the FEM software COMSOL multiphysics. In this, we draw the geometry first, assign appropriate material parameters, apply suitable boundary conditions, mesh the whole volume, and run the software for computation. We drew a rectangle of 50 μm $\times$ 50 μm $\times$ 10 mm and assigned the material parameters of air with refractive index 1. In the middle of 10 mm length of this rectangle, we drew a 50 μm $\times$ 50 μm $\times$ 1 mm rectangle and assigned the material parameters of GaAs with refractive index 3.6. On top of the GaAs, we drew a rectangle of length, width, and height as shown in figure 1a. We assigned the material parameters of gold for this with a conductivity of 31 $(\mu\Omega m)^{-1}$. We used periodic boundary conditions for the sides (50 μm $\times$ 50 μm) and port boundary conditions for THz excitation and de-excitation at the left and right surfaces of 10 mm long rectangle. The electric field of the light wave excited at the left port is

$$E = (\cos\theta\hat{x} + \sin\theta\hat{y}) \exp[i(kz - \omega t)],$$

where $k = 2\pi/\lambda$ and ω is the angular frequency of the light wave. Here, xy is the plane in which the GaAs substrate lies and z direction is along the 10 mm side of the rectangle. The whole geometry is meshed with the size of about one third of the wavelength of the THz wave in air, one sixth of the wavelength in GaAs, and one tenth of the wavelength in gold. The software is run to calculate the S parameters. S_{21} gives the ratio of the amplitude of the transmitted electric field and the incident electric field. Figure 1b shows the power transmission ($|S_{21}|^2$) as a function of THz frequency for $\theta = 0°$ and $90°$

where θ is the angle between the normally incident THz electric field and the length of the wires. For $\theta = 0°$ there is a strong resonance at 1.05 THz and for $90°$ the transmission is the same throughout the spectral range of 0.2–1.75 THz. In a WGP, long wires are in periodic arrangement. When the polarisation of the incident electric field is along the length of the wires, the electric field drives the electrons in the wires for any frequency of the electric field. That is, it works as a polariser for a broad band of frequencies, whereas, when there are cuts in the wires, each gap is working as a capacitor and each cut-wire is working as an inductor with some resistance. Therefore, a single cut-wire has a resonance for driving electrons in the wires just like an LC circuit making it to work as a narrow-band polariser of light. Figure 1c shows the distribution of electric field norm and current density at the resonance for $\theta = 0°$. Black arrow indicates the direction to which all the small red arrows are pointing. The single direction of the current density lines shows that there is an electric dipole in the cut-wires. As there is a resonance for $0°$ and no resonance for $90°$, the device can work as a narrow-band polariser for frequencies around the resonance. For the tunability of this narrow band, we studied the role of the length of the wires in the range of $40-65$ μm with the width and thickness of the wire fixed to be 2 μm and 150 nm, respectively and period of the array is taken to be 50 μm.
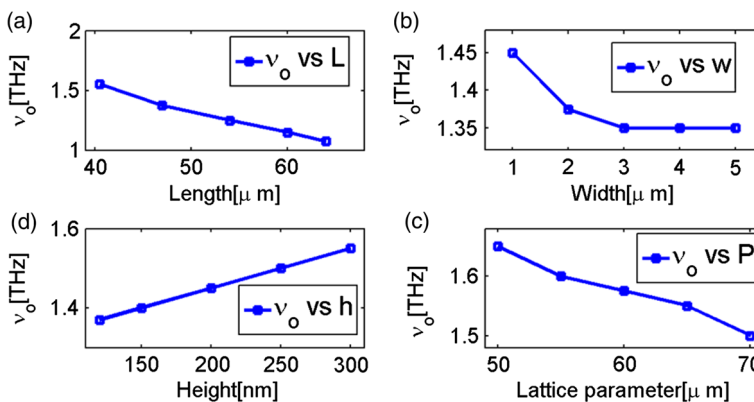
Figure 2a shows the resonance frequency of the wires vs. L of the cut-wires when $w = 2$ μm, $h = 120$ nm, and $P = 50$ μm. Figure 2b shows the resonance frequency of the wires vs. w of the cut-wires when $L = 47$ μm, $h = 120$ nm, and $P = 50$ μm. Figure 2c shows the resonance frequency vs. P of MM when $L = 35$ μm, $w = 2$ μm, and $h = 120$ nm. Figure 2d shows the resonance frequency vs. h of the wires when $L = 47$ μm, $w = 2$ μm, and $P = 50$ μm. These plots show that the tunability of the resonance frequency of the cut-wires is possible by changing w, h of the wires, and P of the unit cell but we considered L alone in experiments because the FEM simulations show better sensitivity for this parameter.

3. Experimental

We fabricated the cut-wire MMs using electron-beam (e-beam) lithography. We prebaked an SI-GaAs substrate at 200°C for 5 min, spin-coated positive photoresist polymethyl methacrylate (PMMA) at 2000 rpm at 400 ramp for 45 s, baked it at 170°C for 6 min, exposed to e-beam over 5×5 mm^2 area with an aperture size of 30 μm, area dosage of 200 μC/cm^2, and acceleration voltage of 20 kV. Then the sample was developed in MIBK : IPA solution for 90 s and UV grade IPA
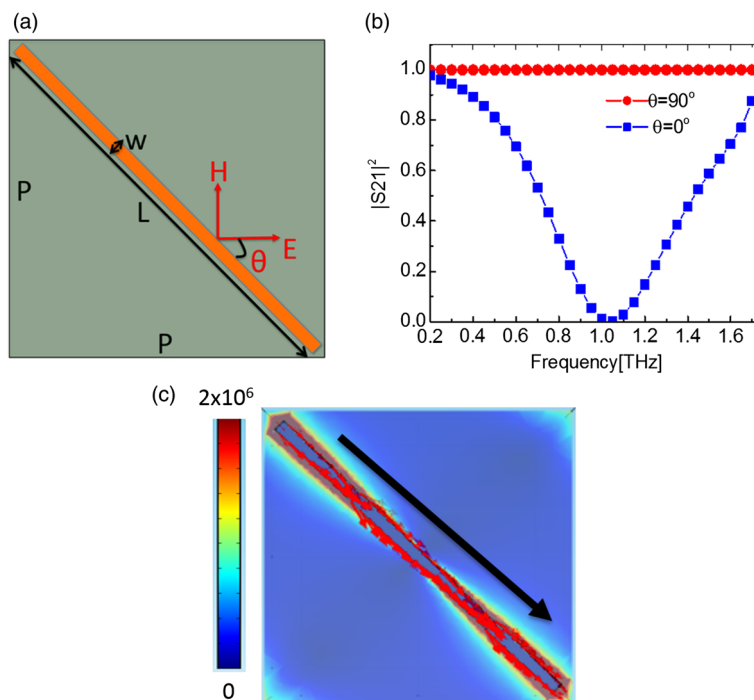
Figure 1. **(a)** Unit cell of the metamaterial: gold cut-wire on the SI-GaAs. Here, $L = 65$ μm, $w = 2$ μm, $P = 50$ μm, and $h = 150$ nm. The angle between the wire axis and the normally incident THz electric field is θ, **(b)** calculated $|S_{21}|^2$ vs. frequency of the metamaterial for $\theta = 0°$ and $90°$, and **(c)** electric field norm (colour plot) and electric current density (arrow) at the resonance for $\theta = 0°$.


Figure 2. **(a)** Resonance frequency vs. length of the cut-wires from FEM simulations, **(b)** resonance frequency vs. width of the wires from FEM, **(c)** resonance frequency vs. lattice parameter from FEM simulation data, and **(d)** resonance frequency vs. height of the wires from FEM.

stopper, and DC sputter with gold for 150 nm thickness. The residual resist was lifted off in acetone bath to get the cut-wire pads on SI-GaAs substrate. We fabricated different samples with different length of cut-wires to experimentally study the dependence of the response on the length of the cut-wire.

We mounted the fabricated sample on a rotatable mount and placed it in a THz time-domain spectroscopy set up with photoconductive antenna source and electro-optic sampling based detection for 0.1–2 THz. We acquired the THz reference waveform before mounting the sample and the sample waveforms after mounting the sample. We acquired sample waveforms for various angles of the MM sample (see figure 3). We truncated the waveforms to 18 psec before the echo from the SI-GaAs substrate arrived such that the Fourier transform would not contain fringes in the spectrum. This gives a spectral resolution of 55 GHz. The ratio of amplitude of transmission spectra through the sample and the reference measured in nitrogen gas ambience is the transmission coefficient and its square is the power transmission.
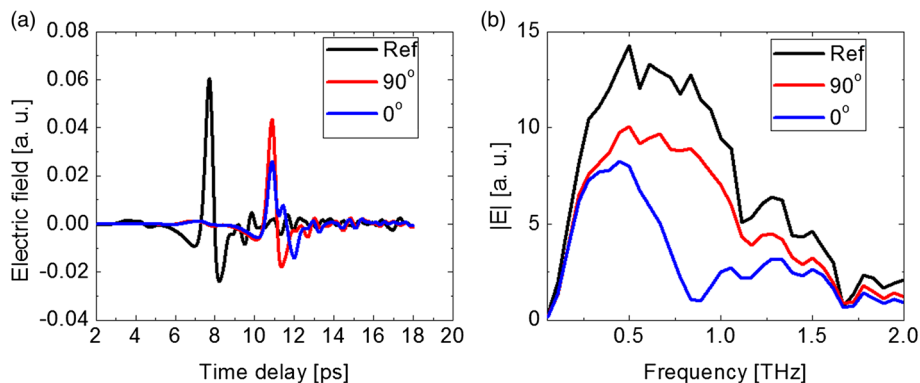
Figure 3. (a) THz waveforms transmitted through the reference, through the single cut-wire MM for angle $\theta = 90°$ and $0°$ and (b) amplitude of the electric field obtained by Fourier transformation of the reference and sample waveforms. We can see an absorption in the spectrum at 0.9 THz for $\theta = 0°$.
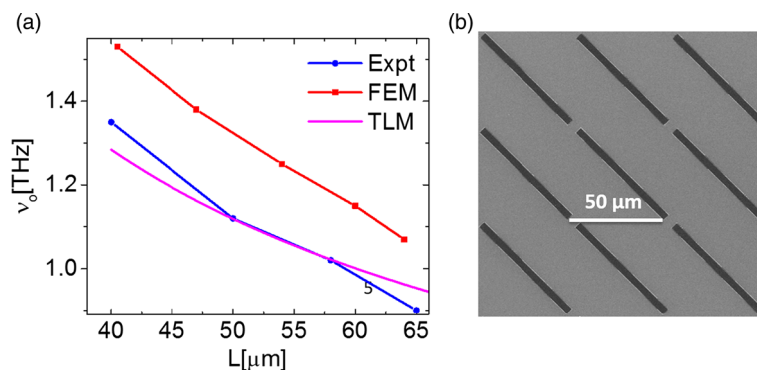
Figure 4. (a) Comparison of the centre frequency of resonance vs. length of the cut-wires from the experimental (Expt) data, FEM data, and TLM and (b) SEM image of the single-wire MM.

4. Results and discussions

After introducing cuts in a continuous WGP, the device which acts as a metal for light of polarisation along the wires will become insulator at some frequencies. This was explained using an LC circuit analogy [32]. We made use of a transmission line model (TLM) [33] to explain the trend of resonance frequency of the cut-wires vs. the frequency. In this model, the cut-wires are modelled as rectangular current-carrying inductor elements and the gap between the wires as capacitance of a parallel plate capacitor. The equation for the resonance frequency of the device in terms of the geometrical parameters as in figure 1a is given by the following equation:

$$\nu_{\text{TLM}} = \left\{ \frac{8\pi^2 Lwh\varepsilon_0}{\sqrt{2}P - L} \left[\ln \frac{2L}{w + h} + 0.5 \right. \right.$$
$$\left. \left. + 0.2235 \left(\frac{w + h}{L} \right) \right] 10^{-7} \right\}^{-1/2}. \quad (1)$$

Here, L, w, and h are the length, width, and height of the cut-wire, and P is the period of the MM lattice. These quantities are in mm and permittivity of free space ε_0 is in F/mm.

We experimentally studied single cut-wire MMs of different lengths and compared them with FEM- and TLM-based values in figure 4a. While there is excellent qualitative agreement between the analytical, simulated, and experimentally measured dependence of resonance frequency on the length of the wire, resonances obtained from finite element are slightly off ($\sim$20%). This may be due to the difference in the material properties used in simulations and the difference between the actual dimensions of the fabricated structures and simulations. Figure 4b shows an SEM image of the cut-wire MM.

As a next step, we realised multiband THz polariser by using multiple cut lines. Figures 5a–5c show the measured power transmission vs. frequency as a function of the angle of the cut-wire MM with single, double, and triple cut-wires respectively in a single unit cell. These were obtained by using MATLABs contour plot function. The single cut-wire MM has a cut-wire with
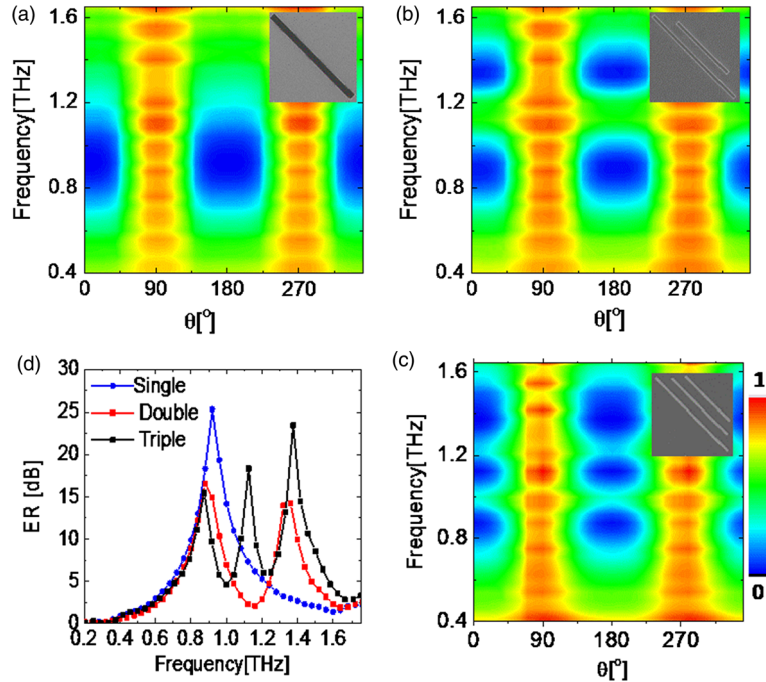
Figure 5. (**a**)–(**c**) The measured normalised transmission coefficient for single, double, and triple narrowband THz polarisers at 0.92 THz, (0.88, 1.36) THz and (0.87, 1.13, 1.37) THz, respectively and (**d**) The plot of ER as a function of frequency for all the three devices.

length, width, and height of 65 μm, 2 μm, and 150 nm, respectively, the double cut-wire MM has an additional cut-wire with length, width, and height of 40 μm, 2 μm, and 150 nm, respectively and the triple cut-wire MM has an additional cut-wire with length, width, and height of 50 μm, 2 μm, and 150 nm, respectively.

The extinction ratio (ER) is defined in terms of the power transmission of the cut-wires along and perpendicular to the wires as follows:

$$ER = 10 \log\left[\frac{T_{90}}{T_0}\right].   \tag{2}$$

Here, T_0 is the power transmission through the MM when $\theta = 0°$ and T_{90} is the power transmission when $\theta = 90°$. Figure 5d shows the plots of ER vs. frequency for the MMs considered here. The ER of the single-band polariser is about 25 dB at 0.92 THz. This means that there is 0.0032 times signal at 0° compared to that at 90° at 0.92 THz. Moreover, there is about 45% loss in the signal after inserting all polarisers at 90°. The ERs of the double-band polariser are 16 and 14 dB around 0.88 and 1.36 THz, respectively. The ERs of the triple-band polariser are 15, 18, and 23 dB, respectively at 0.87, 1.13, and 1.37 THz. The measured ER may increase if the spectral resolution in the THz-TDS measurement is increased further by pushing the echo from the SI-GaAs further in time (using thicker substrate). From the plots

we can see that if the number of cut-wires increases in the unit cell, the widths of the polarisation bands decrease. It should be noted that the bandwidth of each of these polarisers is <0.2 THz (figure 4d). The working mechanism of these polarisers is that the electric field of the resonant frequency component in the incoming THz radiation drives the dipoles in the cut-wires to have dips in the transmission. These polarisers have applications in spatial frequency filtering, in reducing radar cross-section using MM absorbers, reducing interferences in communication systems [34], bio-medical imaging [35], in detection of small fire in forest [36], in polarimetric imaging [37], in sensing of dielectrics [38], etc.

5. Conclusion

We experimentally demonstrated the cut-wire MM-based single and multiband THz narrow-band polarisers. We first used FEM-based simulations to optimise the cut-wire dimensions for specific frequencies. These results showed large dependence of resonance frequency on the length of the cut-wires. Based on these, we have fabricated single-, double- and triple-band polarisers with varying lengths to cover different frequency bands. We further showed that the TLM explains the tunability of the polarisation band with length of the

cut-wires. An ER larger than 15 dB is achieved in the narrow single, double or triple bands. These have potential use in spectroscopic studies as well as in polarimetric and biomedical imaging, and communication networks.

References

[1] F Yan, C Yu, H Park, E P J Parrott, P Pickwell-MacPherson, *J. Infrared Millim. Terahertz Waves* **34**: 489 (2013)

[2] M C George, J Bergquist, R Petrova, B Wang and E Gardner, *Proc. SPIE* **8873**, 887302 (2013)

[3] C-F Hsieh, Y-C Lai, R-P Pan and C-L Pan, *Opt. Lett.* **33**, 1174 (2008)

[4] L Ren *et al, Nano Lett.* **9**, 2610 (2009).

[5] A Wojdyla and G Gallot, *Opt. Express* **19**, 14099 (2011)

[6] D Polley, A Ganguly, A Barman and R K Mitra, *Opt. Lett.* **38**, 2754 (2013)

[7] I Yamada, K Takano, M Hangyo, M Saito and W Watanabe, *Opt. Lett.* **34**, 274 (2009)

[8] A Partanen *et al, Appl. Opt.* **51**, 8360 (2012)

[9] Z Huang, H Park, E P J Parrott, H P Chan and E Pickwell-MacPherson, *IEEE Photon. Technol. Lett.* **25**, 81 (2012)

[10] T Kondo, T Nagashima and M Hang, *J. Appl. Phys.* **42**, L373 (2003)

[11] S-H Lee, S-Y Gee, C Kang and C-S Kee, *J. Opt. Soc. Korea* **14**, 282 (2010)

[12] M P M Colleoni and B Vidal, *Opt. Express* **22**, 30156 (2014)

[13] B R Sangala *et al*, 12*th International Conference on Fiber Optics and Photonics, India* (Optical Society of America, 2014) Paper ID S4D.4

[14] N K Grady *et al*, *Science* **340**, 1304 (2013)

[15] R Yahiaoui *et al,* 35th *International Conference on Infrared, Millimeter, and Teraertz waves* (IEEE, 2010) p. 1

[16] V M Shalaev *et al*, *Opt. Lett.* **30**, 3356 (2005)

[17] V D Lam, N T Tung, L V Hong and Y P Lee, *J. Phys.: Conf. Ser.* **187**, 012015 (2009)

[18] C Imhof and R Zengerle, *Opt. Express* **14**, 8257 (2006)

[19] C Imhof and R Zengerle, *Opt. Commun.* **280**, 213 (2007)

[20] Z Lu, B Camps-Raga, N E Islam, *Phys. Res. Int.* **2012**, Article ID 206879 (2012)

[21] Q-Y Wen *et al*, *Appl. Phys. Lett.* **97**, 021111 (2010)

[22] J Li *et al*, *Appl. Phys. Lett.* **102**, 121101(2013)

[23] H Tao *et al*, *Opt. Express* **16**, 7181 (2008)

[24] T V Do *et al*, *Adv. Nat. Sci. Nanosci. Nanotechnol.* **3**, 045014 (2012)

[25] Y Fan, N-H Shen, T Koschny and C M Soukoulis, *ACS Photon.* **2**, 151 (2015)

[26] T Suzuki, M Nagari and Y Kishi, *Opt. Lett.* **41**, 325 (2016)

[27] A Ferraro *et al*, *Opt. Lett.* **41**, 2009 (2016)

[28] T-Y Yu *et al*, *Opt. Lett.* **42**, 4917 (2017)

[29] X-X Zheng, Z-Y Xiao and X Y Ling, *Opt. Quant. Electron.* **48**, 461 (2016)

[30] B Li *et al*, *AIP Adv.* **6**, 025215 (2016)

[31] M Liu *et al*, *Nature* **487**, 345 (2012)

[32] K Takano *et al*, *J. Appl. Phys.* **107**, 024907 (2010)

[33] L Fu, H Schweizer, H Guo, N Liu and H Giessen, *Phys. Rev. B* **78**, 115110 (2008)

[34] A M H Abadi and N Behdad, *IEEE Trans. Antennas Propag.* **63**, 4766 (2005)

[35] V V Tuchin, L V Wang and D A Zimnykov, *Optical polarisation in biomedical applications* (Springer, Berlin, 2006)

[36] G A Lampropoulos, J Christowski and R M Measures, *Applications of photonic technology* (Springer, Berlin, 1995)

[37] A Watson, *Fabrication of micropolariser and narrow band pass pixel filters for focal plane array* , M.S. thesis (University of Dayton, Ohio, USA, 2011)

[38] C Sabah, B Mulla, H Altan and L Ozyuzer, *Pramana – J. Phys.* **91**: 17 (2018)